Modeling impacts of highly regulated inflow on thermal regime and water age in a shallow reservoir

Binbin Wu, Guoqiang Wang, Changming Liu and Zongxue Xu

ABSTRACT

Thermal regime and transport of dissolved pollutants, strongly related to water quality and algae bloom in reservoirs, may be quantized by indicators of water temperature and water age, respectively, and these indicators are more spatially and temporally variant in shallow reservoirs. Here, a two-dimensional model was used for studying characteristics of the indicators in Douhe Reservoir, based on data of the year 2008. Douhe Reservoir is a typical shallow reservoir in Northern China, characterized by highly regulated inflow and thermal effluent. The impacts of the regulated inflow on reservoir thermal regime and water age were then analyzed through numerical experiments. The results show that the effects of inflow are associated with the flow circulations induced by inflow, thermal effluent, and wind. The most efficient inflows for alleviating thermal pollution and improving water exchange are 32.5 and 19.5 m^3/s, respectively. A positive logarithmic correlation is found between water temperature and water age under the impact of inflow, while thermal effluent and wind have a slightly negative effect on the correlation. These findings provide useful information for better understanding the complex hydrodynamic and mass transport processes in a shallow reservoir.

Key words | inflow, shallow reservoir, temperature, thermal effluent, water age, wind

Binbin Wu
Guoqiang Wang (corresponding author)
Changming Liu
Zongxue Xu
College of Water Sciences,
Beijing Normal University,
Key Laboratory of Water and Sediment Sciences,
Ministry of Education,
Beijing 100875,
China
E-mail: *wanggq@bnu.edu.cn*

Changming Liu
Institute of Geographical Sciences and Natural Resources Research,
Chinese Academy of Sciences,
Beijing 100101,
China

INTRODUCTION

Water temperature is a key factor in physical, biological, and chemical processes of aquatic ecosystems (Cassie 2006; Encina *et al.* 2008; Prats *et al.* 2010; Wang & Xu 2011; Wang *et al.* 2012), and is a crucial element in controlling algae blooms in lakes and reservoirs (Chen *et al.* 1999; Jiang *et al.* 2010). Because of anthropogenic influences, many lakes and reservoirs have altered thermal regimes. Considering all types of anthropogenic perturbations, thermal effluent from power plants has one of the greatest effects on thermal regime alterations (Brezina *et al.* 1970; Cassie 2006), and it can promote algae blooms in lakes and reservoirs (Chen *et al.* 1999). The effect of thermal pollution may be local or extend over a large area, depending on factors such as the difference in water temperature relative to natural conditions, volume of thermal effluent relative to inflow/outflow, and actual volume of the lake or reservoir (Encina *et al.* 2008).

Water age is defined as 'the time that has elapsed since the particle under consideration left the region in which its age is prescribed as being zero' (Delhez *et al.* 1999). It is a useful timescale for quantifying transport properties of dissolved pollutants, and can describe temporal and spatial heterogeneities of mass exchange in lakes and reservoirs (Takeoka 1984; Boynton *et al.* 1995; Delhez *et al.* 1999; Shen & Wang 2007; Li *et al.* 2011). Water age is a function of hydraulic and meteorological factors and water body characteristics. Among the latter, inflow is considered one of the dominant factors controlling transport processes. For shallow lakes and reservoirs, wind also plays an important role (Li *et al.* 2011; Shen *et al.* 2011). The concept of water age has been widely applied to calculate transit time of dissolved pollutants in coastal water areas with intense water exchange induced by tide and wind (Deleersnijder *et al.* 2001; Liu *et al.* 2012). However, there has been little application to shallow lakes or reservoirs with

doi: 10.2166/hydro.2013.178

intense water movement induced by human activities (Li *et al.* 2011). In addition, Straskraba *et al.* (1999) found that mean water residence time is directly related to hydrodynamic, chemical, and biological processes of reservoirs. Water age is representative of residence time (Takeoka 1984; Monsen *et al.* 2002) and is also closely related to water quality (Shen *et al.* 2011), algae growth and phytoplankton distribution (Andrejev *et al.* 2004; Jiang *et al.* 2010; Li *et al.* 2011). Many empirical relationships have been found between phytoplankton and water age (Lucas *et al.* 2009). Water temperature is an important characteristic of surface water systems that may covary with water age, especially if that age is directly governed by freshwater inflow (Lucas *et al.* 2009); however, little research has been done on the existing relationship between water temperature and water age.

Shallow reservoirs are more sensitive to changes in inflow and wind. Accordingly, water temperature and water age tend to be more variant in space and time, especially for shallow reservoirs with thermal effluent. For reservoirs in Northern China, inflows almost entirely control the source of freshwater because of prolonged periods of low rainfall and drought. Most inflows are highly regulated by anthropogenic manipulation, such as water transfer (Liu 1998). Therefore, it is essential for effective reservoir management to understand how regulated inflow influences the thermal regime and transport of dissolved pollutants, and their relationship under the impact of inflow in a shallow reservoir with thermal effluent. The objectives of this paper are to investigate: (1) the impacts of highly regulated inflow on thermal regime and water age, and associated wind effect; and (2) the relationship between thermal regime and water age under the effect of inflow in a shallow reservoir with thermal effluent. A case study was carried out for Douhe Reservoir, a typical shallow reservoir in Northern China, which is influenced by the combined effects of highly regulated upstream inflow and thermal effluent (Sheng *et al.* 1990; Lu *et al.* 2001a, b). The impacts of regulated inflow on thermal regime and water age were investigated by a series of numerical simulations with four representative inflows, and the impacts of wind were also investigated by considering eight directions and three representative speeds. Since transport processes are important in shaping spatial patterns of non-conservative quantities such as water temperature (Lucas *et al.* 2009), the relationship between thermal regime and water age under the influence of regulated inflow was also discussed.

METHODS

Study area

The Douhe Reservoir, about 15 km northeast of the city of Tangshan, is a typical multipurpose, shallow reservoir (Figure 1). It is the first large reservoir in Hebei Province, with regulated storage of 0.0694 km^3 and corresponding water surface area 17.8 km^2 (Sheng *et al.* 1990). The reservoir is in the upper reach of Douhe River, which has two primary tributaries, the Quanshui River and Guan River. The reservoir was built in 1956 for the initial purposes of flood control, irrigation, and industrial water use. Since the construction of a nearby power plant in 1976, it has also served as a cooling pond. Since 1988, it has been used as the final regulating reservoir for a water transfer project from Luan River to Tangshan. The project was developed to transfer water from Luan River to the

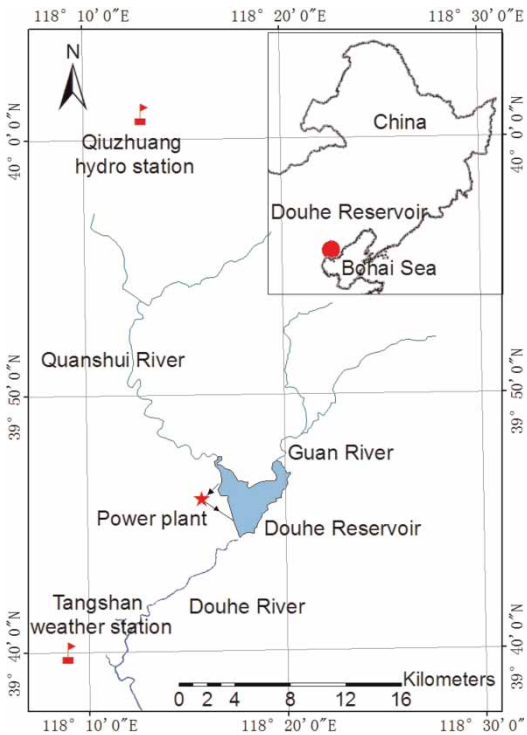

Figure 1 | Location of study area, tributaries, and related stations for Douhe Reservoir, China.

reservoir via Huanxiang River, Qiuzhuang Reservoir and Quanshui River, and to supply drinking water to Tangshan. Inflow to Douhe Reservoir became highly regulated because of this project. The transferred water dominates inflow to the reservoir, representing more than 90% of the inflow over the last decade (2001–2010) (Liu & Cheng 2011). In 2008, the total duration of water transfer was 77 d from late March to early December, and the total volume of transferred water accounted for approximately 88% of the total inflow to the reservoir.

Model description

Douhe Reservoir is a shallow reservoir with water depth ranging from 2 to 12 m and an average depth of about 4 m (He 1997). According to previous research (Li *et al.* 2001), a two-dimensional (2-D) model approach was sufficiently accurate to describe hydrodynamic and water quality processes in this shallow reservoir. Thus, we used the Danish Hydraulic Institute (DHI) 2-D modeling system MIKE21 to simulate thermal regime and water age. The model has been extensively documented for modeling the flow circulation, thermal stratification, sediment transport, water quality, and eutrophication processes in numerous reservoirs, lakes, and estuaries (Warren & Bach 1992; Refsgaard *et al.* 1998; Zhang *et al.* 2011). We used the hydrodynamic (HD) module based on the solution of the 2-D shallow water equations considering temperature evolution for hydrodynamic process simulation. A user-defined ECO lab (a numerical lab for ecological modeling) module was designed for water age simulation, and was coupled with the advection-diffusion module in the hydrodynamic model.

Water age can be computed based on the concentration of a tracer and its age concentration. Transport equations for calculating these concentrations may be written as follows (Delhez *et al.* 1999):

$$\frac{\partial c(t,\vec{x})}{\partial t} + \nabla\left(uc(t,\vec{x}) - K\nabla c(t,\vec{x})\right) + S = 0 \tag{1}$$

$$\frac{\partial \alpha(t,\vec{x})}{\partial t} + \nabla\left(u\alpha(t,\vec{x}) - K\nabla \alpha(t,\vec{x})\right) = c(t,\vec{x}), \tag{2}$$

in which c is the tracer concentration, α is the age concentration of the tracer, u is the velocity, t is the time, $\vec{x}$ is a spatial coordinate, K is the diffusivity tensor, and S is the point source. Then, mean age (water age) of the tracer is calculated from:

$$\alpha(t,\vec{x}) = \frac{\alpha(t,\vec{x})}{c(t,\vec{x})} \tag{3}$$

The tracer concentration and its age concentration were set as state variables, and the mean age was set as a dependent variable in the user-defined ECO lab module. Water age was calculated with specified initial and boundary conditions.

Model setup and experiments

Reservoir bathymetry was specified using a 1:10,000 scale topographical map (Figure 2). A Cartesian computational mesh was generated using the MIKE Zero Mesh Generator. The mesh contained 1,931 cells in the horizontal plane, and one uniform layer along the vertical direction. Of the two tributaries, the Guan River was continuously without flow, so it was treated as land in the model; inflow data were thus derived at the entrance of the Quanshui River. Except for the two tributaries, the power plant takes water for cooling from the reservoir and discharges heated water back into the reservoir. Three other water intakes supply water to Tangshan, the local alkali factory, and Caofeidian Industrial Zone. Because the water intakes for the power plant and Tangshan are only a

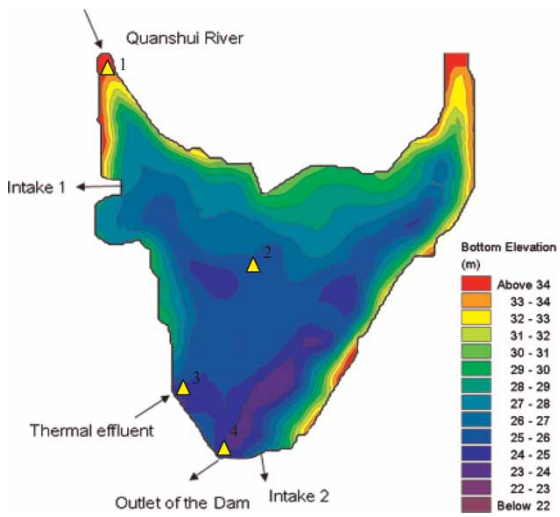

Figure 2 | Bottom elevations (Dagu Height System), boundary locations, and monitoring sites in model domain.

45.5-m distance from each other, they were treated as a single intake and marked as intake 1. Similarly, the water intakes for the local alkali factory and Caofeidian Industrial Zone were combined and marked as intake 2 (Figure 2).

Daily meteorological data, including air temperature, relative humidity, cloud cover and wind, were obtained from the Tangshan weather station. Daily precipitation and evaporation data were derived from Qiuzhuang hydrologic station, 30 km northwest of Douhe Reservoir (Figure 1). In this study, only the data from 2008 were used. Table 1 shows a comparison between the principal meteorological data in 2008 and in the long-term period 1961–2010. The annual average of mean daily air temperature/relative humidity/wind speed, the dominant wind direction, and the average annual precipitation and evaporation were chosen for comparison. The table reveals that most relative errors between meteorological data in 2008 and the 50-year means were less than 4%. The largest relative error (12.5%) was found in wind speed, but the absolute error was still quite small (0.3 m/s). Therefore, the 2008 meteorological data are near average levels, and 2008 was then assumed as a representative year for the study reservoir. During the same year, the power plant pumped thermal effluent into the reservoir at a constant rate every month, while the intakes pumped water out from the reservoir at fixed rates, which were provided by the Douhe Reservoir Administration Bureau. Daily inflows from Quanshui River and outflow to Douhe River were measured for the entire year 2008. Water levels were recorded during water transfer periods. Field sampling was done at four sites during May and November 2008, at intervals of 2–8 d (Figure 2). Field measurements of water temperature were performed onsite, using a portable meter from Yellow Springs Instrument Inc.

The hydrodynamic model was used to simulate the entire year 2008. Surface elevation and temperature initial conditions were set to average values of the first day of the simulation period. A simple linear regression model was used to predict daily water temperatures, based on continuous air temperatures at site 1 (Figure 3; $R^2 = 0.90$). Temperatures of thermal effluents from the power plant are on average 9 °C higher than inflow water temperatures in Douhe Reservoir (Li *et al.* 2001). Therefore, the boundary condition of thermal effluent temperature was generated from the time series of water temperature at site 1. Calibration and validation of the hydrodynamic model were done prior to its application in age and scenario studies.

A series of numerical experiments (22 cases; Table 2) was conducted with respect to tracers discharged into the reservoir via the Quanshui River tributary. Case 1 added the age model to the verified hydrodynamic model, for studying characteristics of the water environment in Douhe Reservoir. For the model setup of water age, passive tracers with a unit concentration (arbitrary units) were continuously released at the Quanshui River entrance, and initial conditions for the tracer and its age concentration were set to zero. Cases 2–5 were developed to study the influence of regulated inflow on thermal regime and water age, without considering wind effects. Based on 2008 data, rates of 6.5, 19.5, 32.5, and 45.5 m^3/s represent low, medium, high, and highest inflows to the reservoir, respectively. Water withdrawals for Tangshan and intake 2 were neglected, because of their small quantities relative to inflow and thermal effluent. Corresponding outflows were assumed equal to the four representative inflows. Cases 6–14 were developed to address the influence of wind (including direction and magnitude) on the inflow effect on thermal regime and water age. Cases 15–18 and 19–22 were designed to distinguish the influences of thermal effluent and wind on the relationship between thermal regime and water age under the impact of inflow, respectively. In all the cases, model configurations and

Table 1 | Comparison of principal meteorological data from 2008 and long-term period (1961–2010, 50 years) at Douhe Reservoir, China

Item	Air temperature[a], °C	Relative humidity[a], %	Wind speed[a], m/s	Wind direction (dominant direction)	Precipitation[b], mm	Evaporation[b], mm
2008	11.5	63.4	2.7	NW	616.6	706.8
50 years[c]	11.6	61.2	2.4	NW	608.7	No data
Relative error	−0.9%	3.6%	12.5%		1.3%	

[a]Annual average of mean daily air temperature/relative humidity/wind speed.
[b]Average annual precipitation and evaporation.
[c]50-year data (1961–2010) from http://cdc.cma.gov.cn/home.do.

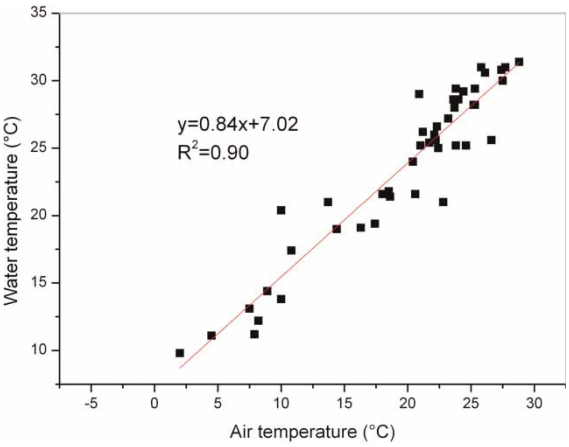

Figure 3 | Relationship between daily air temperature and water temperature at site 1.

parameters, except the driving factors in Table 2, were kept the same as in case 1 (2008 data). Each model was used to simulate 366 d, at a constant time step of 60 s.

Data analysis

Statistical analysis was performed using OriginPro 8.0 software to test differences in modeled water temperatures at different sites. Since daily water temperatures did not follow a normal distribution, the non-parametric Kruskal–Wallis analysis of variance (ANOVA) test was used. Further, the Mann–Whitney test for multiple comparisons was used if the Kruskal–Wallis results showed a significant difference at the 0.05 level. Results were expressed as a median (quartile range, QR).

Regression analysis was applied to determine the relationship between thermal regime and water age using OriginPro 8.0. Because this was the first study examining thermal regime responses to water age variation, an exploratory approach to the data analysis was adopted using a large variety of models. Simple linear, logarithmic, power, and exponential functions were fitted to the data and the coefficient of determination (R^2) was used to discover the model with the best fit.

RESULTS AND DISCUSSION

Model calibration and validation

Field data from 25 March to 30 September 2008 were selected for calibration, and data from 1 October to 31 December 2008 were used for validation. Model calibration and validation were performed at the same sites as field sampling. Water levels at site 4 during water transfer periods and water temperatures at three sites (2, 3, and 4) were used to verify the hydrodynamic model. The main calibrated parameters included time step, bed resistance, horizontal eddy viscosity,

Table 2 | Model experiments for Douhe Reservoir, China

	Flow (unit: m^3/s)				
Scenarios	**Inflow (Quanshui River)**	**Outflow (Douhe River)**	**Thermal effluent**	**Other outflows[a]**	**Wind**
Case 1	2008 data	2008 data	2008 data	2008 data	2008 data
Case 2	6.5	6.5	2008 data	No flow	No wind
Case 3	19.5	19.5	2008 data	No flow	No wind
Case 4	32.5	32.5	2008 data	No flow	No wind
Case 5	45.5	45.5	2008 data	No flow	No wind
Cases 6–13	19.5	19.5	2008 data	No flow	Wind speed 3 m/s, wind directions are E, SE, S, SW, W, NW, N, NE, respectively
Case 14	19.5	19.5	2008 data	No flow	NW 6 m/s
Cases 15–18	Same as cases 2–5	Same as cases 2–5	No flow	No flow	No wind
Cases 19–22	Same as cases 2–5	Same as cases 2–5	2008 data	No flow	2008 data

[a]Other outflows represent water supplies for Tangshan, local alkali factory, and Caofeidian Industrial Zone. Water withdrawals for intake 1 were considered equal to thermal effluent, and withdrawals for intake 2 were neglected in cases 2–22.

and several parameters related to temperature. Based on the Courant–Friedrichs–Lewy condition, a 60-s time step was used to run the model to assume the stability of the adopted numerical scheme, and the critical Courant–Friedrichs–Lewy number was set as 0.8. Manning's roughness coefficient was set to 0.03 s/m$^{1/3}$, and the dimensionless viscosity parameter in the Smagorinsky (1963) formula was set to a constant value of 0.2 for the horizontal turbulence model (Berntsen 2002). To adapt to water level fluctuations, a moving water surface boundary was applied in the model by assigning a threshold value of the water depth to identify dry elements (0.005 m) together with the wetting/drying procedure of Zhao *et al.* (1994) and Sleigh *et al.* (1998).

Modeled and observed water levels showed good agreement in both calibration and validation periods (Figure 4(a) and Table 3), with small mean absolute errors (≤0.06 m), small mean relative errors (<0.2%), and high R^2 (≥0.95). These demonstrated that the hydrodynamic model adequately simulated surface fluctuations caused by variations in wind, precipitation, evaporation, freshwater discharge, and water removal. The heat budget reproduced temporal and spatial variation of reservoir water temperature quite well, with the highest temperature at site 3 and similar temperatures between sites 2 and 4 (Figure 4(b) and Table 3). In the calibration period, mean absolute error, mean relative error, and R^2 were respectively as follows: 0.80 °C, 2.95%, and 0.90 at site 2; 1.76 °C, 3.08%, and 0.84 at site 3; 2.69 °C, 3.87%, and 0.78 at site 4. In the validation period, the model slightly underestimated water temperature at three sites. This was caused by the assumption of fixed excess temperature (9 °C) of thermal effluent to inflow. This temperature is variable in reality, and the winter value in Douhe Reservoir may be higher than 9 °C (Sheng *et al.* 1990). For a more accurate simulation, measured thermal effluent data should be available. In general, however, the hydrodynamic model showed satisfactory performance and was sufficiently accurate for age and scenario studies.

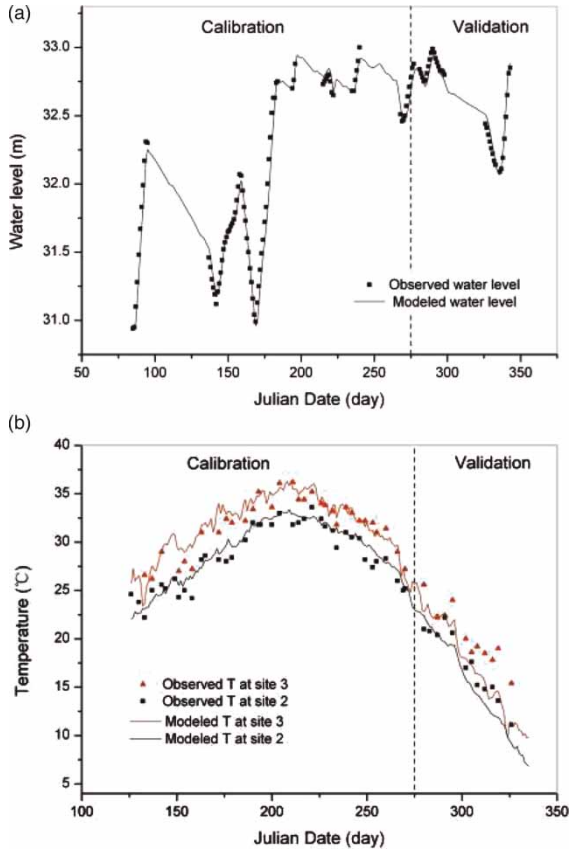

Figure 4 | Time series of modeled (solid line) and observed (dotted points) data in 2008: (a) water level at site 4; (b) temperature at sites 2 and 3.

Characteristics of water environment in the study reservoir

Flow circulations in the reservoir

Water movement in a shallow reservoir like Douhe Reservoir is complex and strong because of the interaction of hydraulic and meteorological factors and characteristics of the reservoir itself. Results show that the flow circulation changed with variable forcings, and was particularly influenced by the competition between inflow and thermal effluent, along with wind effects. For example, when inflow was negligible, the typical flow circulation was driven by thermal effluent with two stable gyres rotating clockwise. One gyre was small and near the hot water effluent. The other spread along the west bank from south to north and supplied water to intake 1, then spread over the entire reservoir (Figure 5(a)). As inflow gradually increased, it disrupted the large original gyre in the northwest (Figure 5(b)). With greater inflow, it began to supplement water to intake 1 and generated an anticlockwise gyre in the northwest part of the reservoir (Figure 5(c)); this expanded with the inflow increase. Results also reveal that outflow only changed flow circulation locally because of its short duration and small discharge in 2008. However, when wind was of a suitable direction and sufficient magnitude, it changed the

Table 3 | Traditional statistical results of calibration and validation for Douhe Reservoir

	Calibration				Validation			
Item	WL	T_2	T_3	T_4	WL	T_2	T_3	T_4
Number of observations	83	39	32	30	37	12	11	11
Mean absolute error, m or °C	0.06	0.80	1.76	2.69	0.05	1.57	2.47	2.70
Mean absolute relative error, %	0.19	2.95	3.08	3.87	0.15	9.68	12.96	13.30
R^2	0.98	0.90	0.84	0.78	0.95	0.82	0.58	0.78

WL represents water level; T_2, T_3, and T_4 represent water temperatures at sites 2, 3, and 4, respectively.

path of freshwater movement (Figure 5(d)). During the entire simulated year (2008), thermal effluent-dominated flow circulation (similar to Figure 5(a)) had a high frequency (around 64%), suggesting that reservoir hydrodynamics were strongly influenced by thermal effluent. Apart from hydraulic and wind-induced flow circulation, density-induced flow circulation is also present in Douhe Reservoir. However, the influence of this flow circulation is less and difficult to determine because of the shallow water depth and 2-D assumption. In general, under the integrated effect of these factors, four typical flow circulations were found in the reservoir, forced by inflow, thermal effluent, and wind.

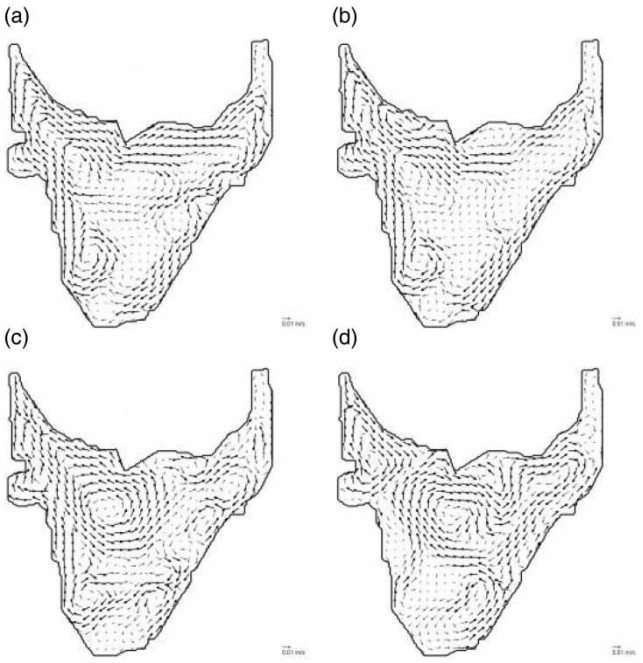

Figure 5 | Four typical circulations in Douhe Reservoir during 2008: (a) day 208, (b) day 196, (c) day 177, and (d) day 341.

Thermal regime

The reservoir thermal regime deviates from natural water temperatures, because of the influence of thermal effluent. Statistical results indicate that water temperature was significantly different at the six reservoir sites (sites 1–4 and intakes 1–2) in 2008 (Kruskal–Wallis ANOVA, $p < 0.01$). Further pairwise comparisons (Mann–Whitney; Table 4) reveal that site 3 and intake 1 were always significantly warmer ($p < 0.01$) than the other sites, exceeding the temperature at site 1 (considered the inflow temperature) by 4–10 °C and 2–8 °C, respectively. This is because northward movement of hot water is constantly maintained by a large withdrawal at intake 1. There was no significant difference ($p > 0.05$) in temperature between site 1 and the other three sites. Results also show that summer was significantly the warmest season ($p < 0.01$), regardless of site. In summer only, water temperatures at all sites were significantly higher than those at site 1 ($p < 0.01$; Table 4), suggesting that summer had the most serious thermal pollution across the

Table 4 | Statistical results of water temperature T at different sites in 2008 (in °C (median (QR)) in Douhe Reservoir

Sites	T_{whole}	T_{sum}
Site 1	16.25 (5.98–26.02)	28.28 (26.52–30.11)
Site 2	18.19 (6.55–28.19)	31.15 (29.41–32.45)[a]
Site 3	22.78 (10.36–31.84)[a]	33.88 (32.72–35.18)[a]
Site 4	17.26 (5.84–27.30)	30.59 (28.79–31.80)[a]
Intake 1	20.61 (7.04–29.79)[a]	32.63 (31.01–34.00)[a]
Intake 2	17.32 (5.76–27.34)	30.64 (28.65–31.82)[a]

T_{whole}: water temperature for entire year 2008.
T_{sum}: water temperature for summer 2008.
[a]Represents significant difference with $p < 0.01$, relative to site 1.

entire reservoir. This may be explained by weaker heat dissipation, stronger radiation (Lu *et al.* 2001b), and greater thermal effluent in summer relative to other seasons. In addition, summer temperatures are generally within the preferential range for algae growth (25–35 °C; Chen *et al.* 1999; Jiang *et al.* 2010), and hence the reservoir faces a high risk of algae blooms in that season.

Four days corresponding to the four typical flow circulations were selected to study the spatial distributions of water temperature. Day 208, with thermal effluent-dominated flow circulation, had the highest temperature in 2008 (Figure 6(a)). The highest temperature was near the hot water effluent and regions with $T > 36$ °C accounted for 2% of the total water surface area, which could threaten aquatic life. As inflow increased (from day 196 to day 177), temperature contours moved from north to south (cf. Figures 6(b) and (6c)), consistent with corresponding flow circulations (Figures 5(b) and 5(c)). For day 341 with flow circulation disrupted by wind (Figure 5(d)), the spread of cold inflow to the middle reservoir was impeded (Figure 6(d)). In general, thermal propagation followed the movement of thermal effluent in the reservoir.

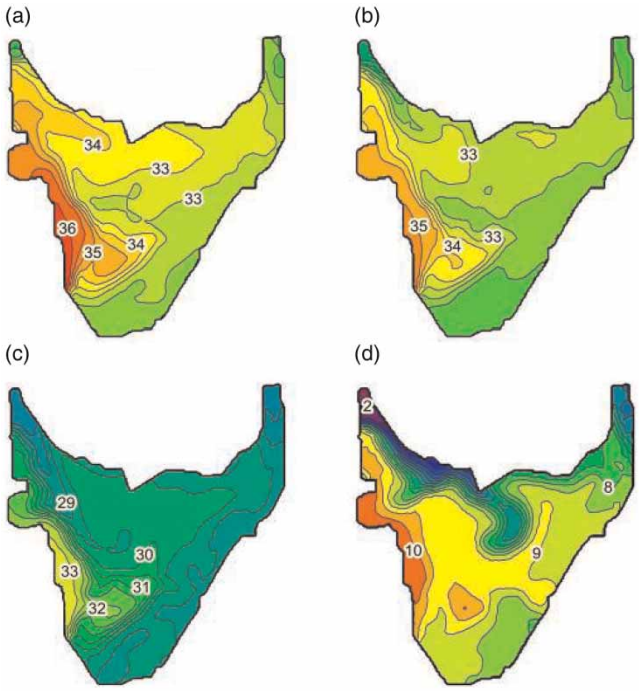

Figure 6 | Water temperature in four typical circulations in Douhe Reservoir during 2008: (a) day 208, (b) day 196, (c) day 177, and (d) day 341.

Water age

Water age at any location of Douhe Reservoir may be used to represent the average time elapsed for parcel transport from the Quanshui River entrance. Time series of water age at different sites showed a similar trend with age, changing with time and location (Figure 7). Water age increased over time (until approximately day 23 at site 2, day 30 at site 3, day 29 at site 4, day 20 at intake 1, and day 28 at intake 2, respectively), suggesting that water brought in by the inflow via the Quanshui River did not reach any of the sites until those days. After that, water ages varied over a very wide range, from approximately 8–125 d. Large fluctuations in water age were caused by the variable inflow and other forcing conditions in 2008. Large declines generally kept pace with water transfer periods, suggesting that the highly regulated inflow had a strong impact on water age in the reservoir. Site 3 tended to have the highest water age, because of the difficulty of refreshing with fresh water due to the effect of the thermal effluent. Site 4 and intake 2 had similar but slightly lesser water ages as site 3, because of their proximity to such a site. The relative magnitudes of water age between intake 1 and site 2 changed with the variable forcings.

Concerning spatial distributions of water age, both homogeneity and heterogeneity were found in the reservoir in 2008. The former was found in thermal effluent-dominated flow circulations, because of the mixing effects of thermal effluent and wind. For example, day 208 had nearly the same age

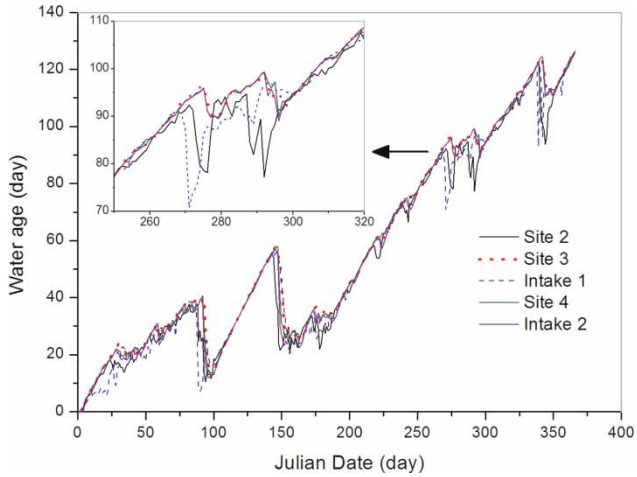

Figure 7 | Temporal variation of water age at different sites in Douhe Reservoir during 2008.

(50 d) as the entire reservoir, except for areas near the Quanshui River entrance (Figure 8(a)). The latter was found in circulations dominated by both inflow and thermal effluent, and the spatial distribution varied according to competition between inflow and thermal effluent. For example, water ages on day 196 (Figure 8(b)) and day 177 (Figure 8(c)) had a similar range (from 0 to 40 d), but the distributions were very different. Day 196 showed local spatial heterogeneity, with lowest ages at the Quanshui River entrance and increasing ages along the north bank, suggesting that dissolved pollutants tend to flow along the north bank. Day 177 had greater spatial heterogeneity compared with day 196, and water age contours moved from the north to west bank and to the entire reservoir. This is because competitiveness of inflow was enhanced on this day, with greater inflow discharge and less thermal effluent. For the flow circulations altered by wind, age distributions were divided by thermal effluent under the effect of wind (Figure 8(d)). Spatial distributions of water age for all such days were generally consistent with the corresponding circulations, and followed the path of freshwater movement.

Regions associated with high water ages are more vulnerable to eutrophication effects (Andrejev *et al.* 2004). Present simulation results support this assertion. There were three algae blooms in areas near the outlet during the summers of 2007–2009, although areas near the thermal effluent release point had slightly higher water ages than this outlet, which should be most ecologically vulnerable. However, very high temperatures (e.g., exceeding 35 °C; Lu *et al.* 2001b) and high velocities might inhibit algae growth. Moreover, when inflow is negligible, most reservoir areas would have substantial risk of algae bloom with high water ages.

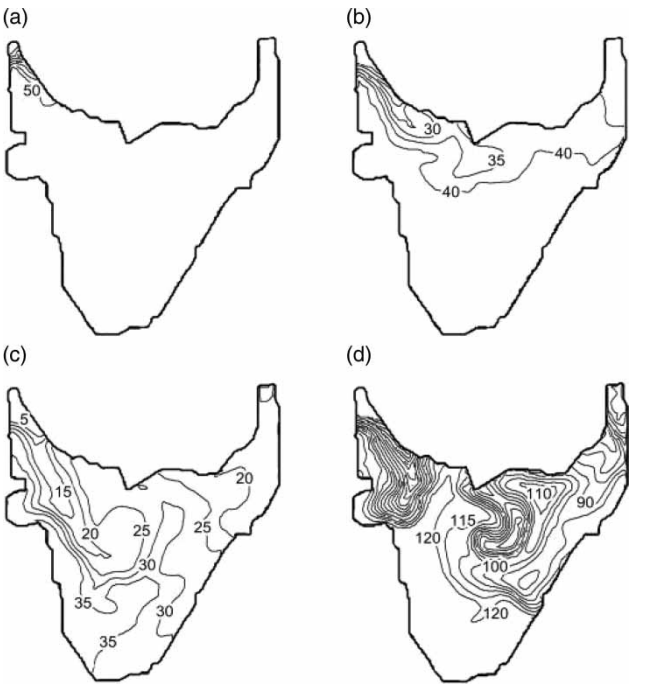

Figure 8 | Water age in four typical circulations in Douhe Reservoir during 2008: (a) day 208, (b) day 196, (c) day 177, and (d) day 341.

Influence of regulated inflow on thermal regime and water age

Inflow to the Douhe Reservoir is highly regulated, mainly controlled by the water transfer project. Analysis of the water environment characteristics above reveals that regulated inflow has strong effects on thermal regime and water age. Hence, cases 2–5 with four representative inflows were examined to access the quantitative effect of highly regulated inflow on thermal regime and water age.

Summer, with the significantly highest water temperature ($p < 0.01$) and greatest occurrence of algae bloom, was chosen to study the effect of inflow on thermal regime. Results reveal that an increase of inflow improved heat exchange between cold inflow and hot thermal effluent, thereby decreasing water temperature. Statistically, when inflow reached 32.5 m^3/s, summer water temperatures for sites 2 and 4 and intakes 1 and 2 dropped significantly in comparison to those with inflow 6.5 m^3/s ($p < 0.01$; Table 5). Spatial distribution on day 208, with the highest temperature, showed similar results. The percentages of areas with temperatures warmer than 36 °C were 1.65, 1.44, 0.74, and 0.11% for corresponding inflows of 6.5, 19.5, 32.5, and 45.5 m^3/s (Figure 9). When inflow increased from 6.5 to 45.5 m^3/s in increments of 13 m^3/s, those percentages decreased by 0.21, 0.70, and 0.63%. These results suggest that maximum inflow efficiency for reducing temperature at most sites and over the entire reservoir was 32.5 m^3/s. However, statistical results also show that temperatures at sites 2 and 4 and intakes 1 and 2 in summer were still significantly warmer than those at site 1, even with inflow 45.5 m^3/s ($p < 0.01$). Indeed, temperatures at site 3 showed no significant decrease when inflow increased from 6.5 to 45.5 m^3/s. These results suggest that it is difficult to eliminate the influence of thermal effluent in summer, but an increase of inflow substantially reduces temperature and alleviates thermal

Table 5 | Statistical results of summer water temperature T at different sites in cases 2–5 (in °C (median (QR))

Inflow, m^3/s	6.5	19.5	32.5	45.5
Site 2	31.64 (30.64–33.08)	30.96 (29.94–32.52)	30.30 (29.24–31.80)[a]	29.87 (28.70–31.07)[a]
Site 3	33.45 (32.39–34.99)	33.51 (32.32–34.94)	33.37 (32.18–34.71)	33.20 (31.93–34.37)
Site 4	31.15 (29.86–32.51)	30.93 (29.92–32.46)	30.55 (29.52–32.08)[a]	30.13 (29.06–31.58)[a]
Intake 1	32.94 (31.83–34.37)	32.62 (31.50–33.86)	32.28 (31.13–33.44)[a]	31.98 (30.66–22.02)[a]
Intake 2	31.14 (29.92–32.54)	30.90 (29.86–32.36)	30.47 (29.43–31.98)[a]	29.99 (28.97–31.46)[a]

[a]Represents a significant difference with $p < 0.01$, relative to inflow of 6.5 m^3/s.

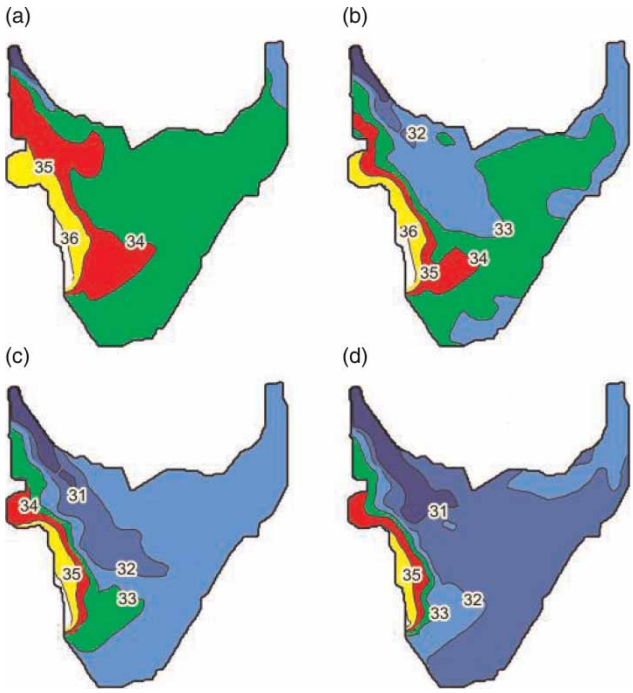

Figure 9 | Influence of inflow on thermal regime for different scenarios on day 208: (a) case 2, (b) case 3, (c) case 4, and (d) case 5.

pollution. In addition, with inflow between 6.5 and 45.5 m^3/s, summer temperatures in the reservoir are still within the preferential range for algae growth (25–35 °C). Thus, inflow could not greatly alleviate algae bloom via decreasing temperature for inflows less than or equal to 45.5 m^3/s.

For water age, steady state (after fresh water reached all reservoir areas) was attained before the end of the 1-year simulation, in all cases. Thus, average water ages at different sites in steady state and the spatial distribution on day 366 were used to investigate the effect of inflow on transport properties. Results reveal that an increase in flow discharge accelerated the transport and discharge of dissolved pollutants from the reservoir. For example, water ages at site 4 and intakes 1 and 2 were very close to that at site 3, with inflow 6.5 m^3/s. As inflow increased to 19.5 m^3/s, water ages at intake 1 began to vary significantly from site 3 (Figure 10). This is because the flow circulation with inflow 6.5 m^3/s is similar to Figure 5(b), which makes it very difficult for fresh water to reach intake 1. The circulation with inflow 19.5 m^3/s is closer to Figure 5(c), in which fresh water more readily reached intake 1. The biggest decreases of water age at all sites were when inflow increased from 6.5 to 19.5 m^3/s. Spatial analysis for day 366 showed the same results. The percentage of areas with water ages less than 50 d was only 1.85% at inflow 6.5 m^3/s; however, it increased to 100% at 19.5 m^3/s (not shown). These results reveal that the maximum inflow effect on water age was at 19.5 m^3/s, and increased inflow does not necessarily generate more efficient water exchange. This is similar to the findings of Li *et al.* (2011). Since water age is closely associated with algae bloom, the regulated inflow is important for reducing the possibility of algae blooms by decreasing water

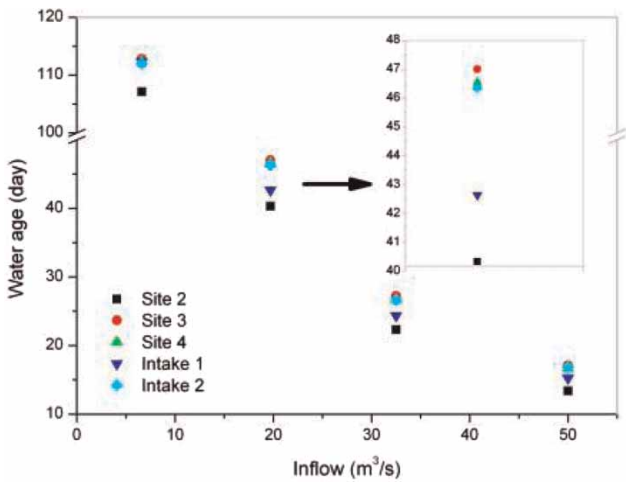

Figure 10 | Influence of inflow on water age for different scenarios (cases 2–5).

age in the reservoir. Nevertheless, with the advance of society and intensification of human activities, the Luan River is also facing eutrophication problems (Domagalski *et al.* 2007). If pollution continues, inflow transferred from this river may become the most important pollution source for Douhe Reservoir in the future. Under that condition, the less the water age is, the greater the algal concentration will be (Li *et al.* 2011). Thus, integrated catchment management (Xia *et al.* 2007) that includes the entire route of the water transfer project is needed.

Cases 3 and 6–14 were also used to investigate the impacts of wind in this shallow reservoir. Results show that wind direction had only a slight impact on water temperature ($p > 0.05$; Figure 11) with a constant speed of 3 m/s, but wind speed had a strong influence ($p < 0.01$; Figure 11) through altering the heat exchange between water and air. Since long-term average wind speed in the study area is less than 3 m/s (Table 1), the average temperature difference caused by wind speed would be around 1 °C or less (Figure 11). For water age, the maximum difference among different wind directions is about 10 d. Northwesterly was found to be the optimum wind direction for enhancing water exchange in the southwest part of the reservoir, which is the area of greatest concern for intakes (Figure 12(a)). This is mainly because this direction is aligned with the inflow, so the effect of wind in this direction is equivalent to increasing inflow speed. Consequently, under this direction, wind speed was also important for water age distribution (Figure 12(b)). In general, the higher the wind speed is, the greater the water exchange is. The average difference in water

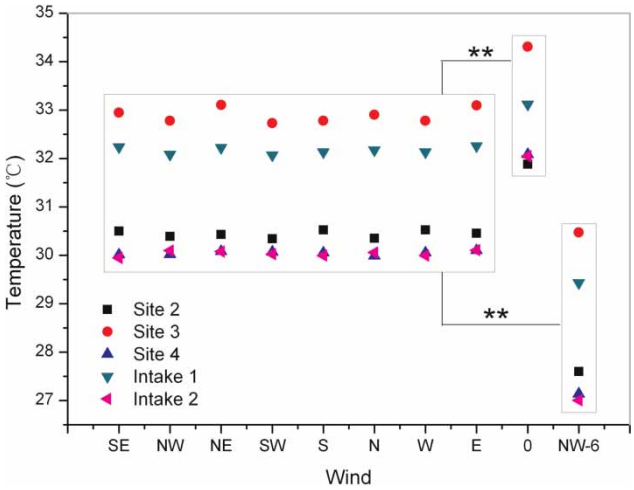

Figure 11 | Influence of wind on thermal regime at different sites.

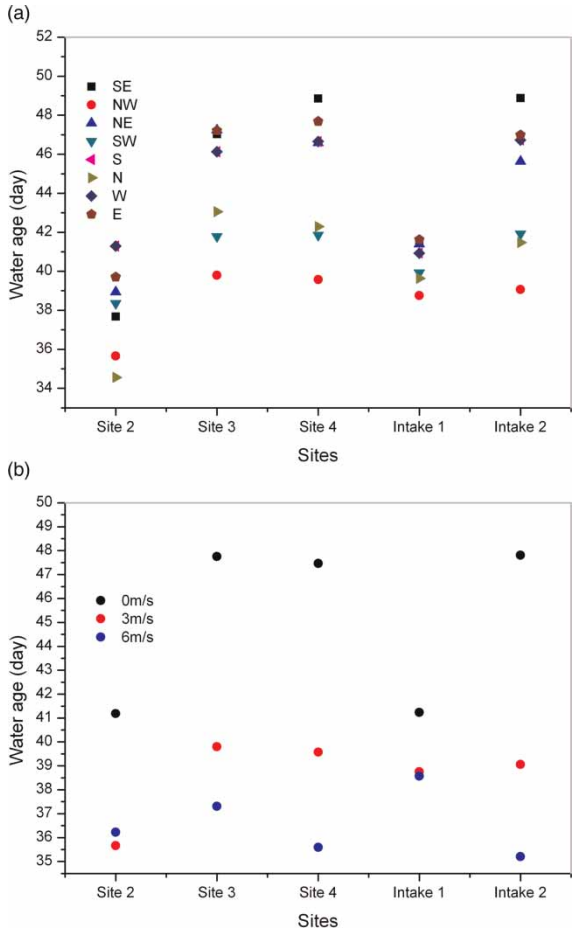

Figure 12 | Influence of wind on water age at different sites: (a) wind direction; (b) wind speed.

age caused by wind speed (with long-term average values less than 3 m/s) would be less than 10 d (Figure 12(b)), equivalent to the change caused by wind direction. Cases 3 and 6–14 all had inflow 19.5 m^3/s, which was the mean discharge for inflow in 2008. Average water age in the reservoir with inflow 19.5 m^3/s was 45 d (Figure 10), so the change caused by wind (<10 d) would influence the impacts of inflow on water age.

Relationship between thermal regime and water age under the impact of inflow

The above analysis of the influence of regulated inflow shows that 32.5 and 19.5 m^3/s were the most efficient inflows for reducing water temperature and water age, respectively. This indicates that water age is more sensitive to changes in flow circulation induced by inflow than is water temperature.

This is reasonable because inflow is decisive for the calculation of water age according to its definition (Delhez *et al.* 1999). However, the determining factor of water temperature in shallow reservoirs is not inflow, though it is also a very important factor in influencing the heat balance, but the heat exchange between water and air. This also indicates that water age can influence the thermal regime. Li *et al.* (2010) found that thermal regime could also affect water age through density-induced flow circulation. In a shallow reservoir like Douhe, however, the effect of thermal regime on water age via density-induced flow circulation is very small, so that the relationship here principally reflects the influence of water age on thermal regime. Consequently, for explicitly assessing the impact of water age on thermal regime, the effect of air temperature variation should be excluded or weakened. Here, the quantitative relationship between thermal regime and water age was studied using the maximum water temperature in summer and average water age in steady state in cases 2–22.

Regression analysis results show that a logarithmic function produced the best fit for the relationship in the reservoir (Table 6). The general formula can be expressed as:

$$Y = a \ln X + b \tag{4}$$

where X and Y represent water age and maximum water temperature at different sites within cases 2–22, respectively; a and b are parameters. As given in Table 6, a is always larger than zero for all functions, so maximum water temperature increases gradually with water age. This is reasonable because greater water age means poorer water exchange with the external environment, leading to heat accumulation and warmer water temperature in the reservoir (Lucas *et al.* 2009). Coefficients of determination (R^2) are also listed in Table 6, and can be used

Table 6 | Relationships between thermal regime (Y = maximum water temperature) and water age (X) in cases 2–22

Case	Site	R^2	Function	
Different inflows	Cases 2–5 (with thermal effluent, without wind)	Site 2	0.99	$Y = 1.30\ln X + 28.75$
		Site 3	0.72	$Y = 0.52\ln X + 33.38$
		Site 4	0.92	$Y = 0.91\ln X + 30.05$
		Intake 1	0.97	$Y = 0.88\ln X + 31.08$
		Intake 2	0.94	$Y = 0.96\ln X + 29.86$
		All sites	0.68	$Y = 1.27\ln X + 29.23$
	Cases 15–18 (without thermal effluent and wind)	Site 2	0.99	$Y = 0.82\ln X + 27.77$
		Site 3	0.98	$Y = 0.86\ln X + 27.71$
		Site 4	0.96	$Y = 0.78\ln X + 28.13$
		Intake 1	0.98	$Y = 0.90\ln X + 27.22$
		Intake 2	0.99	$Y = 0.64\ln X + 28.76$
		All sites	0.91	$Y = 0.90\ln X + 27.57$
	Cases 19–22 (with thermal effluent and 2008 wind)	Site 2	0.87	$Y = 1.04\ln X + 29.11$
		Site 3	0.80	$Y = 0.38\ln X + 33.80$
		Site 4	0.89	$Y = 0.64\ln X + 30.45$
		Intake 1	0.97	$Y = 0.72\ln X + 31.56$
		Intake 2	0.89	$Y = 0.78\ln X + 29.85$
		All sites	0.23	$Y = 0.76\ln X + 30.76$
Different winds	Cases 6–13 (different wind directions)	Site 2	0.58	$Y = 0.84\ln X + 27.83$
		Site 3	0.37	$Y = 1.21\ln X + 26.41$
		Site 4	0.16	$Y = 0.19\ln X + 29.19$
		Intake 1	0.58	$Y = 2.25\ln X + 24.59$
		Intake 2	0.28	$Y = 0.49\ln X + 30.62$
		All sites	0.40	$Y = 0.75\ln X + 29.03$
	Cases 3, 11, and 14 (different wind speeds)	Site 2	0.61	$Y = 19.26\ln X - 38.51$
		Site 3	0.75	$Y = 14.62\ln X - 18.54$
		Site 4	0.95	$Y = 17.47\ln X - 30.46$
		Intake 1	0.68	$Y = 40.63\ln X - 108.35$
		Intake 2	0.74	$Y = 16.53\ln X - 26.86$
		All sites	0.73	$Y = 20.31\ln X - 39.22$

to assess the degree of impact of water age on thermal regime. Under the influence of inflow, best correlations were found in cases without thermal effluent and wind (cases 15–18), with an average R^2 of 0.98. The difference of relationships between thermal regime and water age at five sites was small, and all sites could be expressed by one equation ($R^2 = 0.91$). Although thermal effluent (cases 2–5) had a slight effect on decreasing the correlation (with an average R^2 of 0.91) and magnifying the difference at the five sites, the relationship for all sites could still be expressed by one equation ($R^2 = 0.68$). The wind distribution in 2008 (cases 19–22) also had a negative effect on the correlations, giving an average R^2 of 0.88. This value is still very high and indicates the importance of water age on thermal regime variation under the impact of inflow. In fact, the relationship between thermal regime and water age indirectly reflected the influence of inflow on the heat balance of the reservoir. The addition of thermal effluent to the system obviously reduced the relative contribution of inflow to the heat balance. Wind enhances heat exchange between water and air, which may also reduce the influence of inflow on the heat balance and affect the correlation. Wind influenced the inflow effects on thermal regime and water age in the reservoir. However, wind in 2008, which approximated the normal wind distribution in the study area (Table 1), would not change the logarithmic relationship between thermal regime and water age under the impact of inflow. Although a low R^2 was found in cases 3 and 6–14 with different wind direction (with an average R^2 of 0.39) and speed (with an average R^2 of 0.75), it was mainly caused by the small range of water age with the fixed inflow of 19.5 m^3/s in those cases, which limited the exhibition of the relationship and decreased the R^2. Overall, a positive logarithmic correlation was found between thermal regime and water age in this shallow reservoir under the impact of regulated inflow, whereas thermal effluent and wind had a slight negative effect on the correlation.

CONCLUSION

Water temperature and water age, which are strongly related to water quality and algae bloom in reservoirs, are considered appropriate indicators of thermal regime and transport processes of dissolved pollutants, respectively. These indicators tend to be more spatially and temporally variant in shallow reservoirs because of the influences of inflow and wind, especially for such reservoirs with thermal effluent. Regulated inflows are major freshwater sources for many reservoirs in Northern China. In this study, the impacts of highly regulated inflow on thermal regime and water age, as well as their relationship under the impact of inflow, were investigated for Douhe Reservoir. This is a typical Northern China shallow reservoir, affected by highly regulated inflow and thermal effluent. The effects of inflow were intimately associated with flow circulations induced by inflow, thermal effluent, and wind. The most efficient inflows for alleviating thermal pollution and improving water exchange were 32.5 and 19.5 m^3/s, respectively, at both intakes and across the entire reservoir. The effects of inflow in the reservoir were modulated by wind. A northwesterly wind can improve water quality by reducing water age at the reservoir intakes. Average changes of water temperature and water age under inflow 19.5 m^3/s caused by wind were less than 1 °C and 10 d, respectively. Finally, a positive logarithmic correlation was found between thermal regime and water age under the impact of regulated inflow, whereas thermal effluent and wind had a slight negative effect on the correlation. This work provides a numerical tool to support adaptive management of Douhe Reservoir by regional water resources and reservoir managers. The relative importance of inflow and wind on thermal regime and water age, and the most efficient inflows for alleviating thermal pollution and improving water exchange may be different in another shallow reservoir. The same is true of the influence of wind (the degree of impact and the optimal wind direction) and the specific function between thermal regime and water age. However, the positive logarithmic relationship of transport processes on thermal regime may serve as a reference for other reservoirs, especially inflow-dominated shallow ones.

ACKNOWLEDGMENT

This research was supported by the National Natural Science Foundation of China (Grant No. 41001155).

REFERENCES

Andrejev, O., Myrberg, K. & Lundberg, P. 2004 Age and renewal time of water masses in a semi-enclosed basin – application to the Gulf of Finland. *Tellus A* **56** (5), 548–558.

Berntsen, J. 2002 Internal pressure errors in sigma-coordinate ocean models. *J. Atmos. Ocean. Technol.* **19** (9), 1403–1414.

Boynton, W. R., Garber, J. H. & Summers, R. 1995 Inputs, transformations, and transport of nitrogen and phosphorus in Chesapeake Bay and selected tributaries. *Estuar. Coasts* **18** (1), 285–314.

Brezina, E. R., Campbell, R. S. & Whitley, J. R. 1970 Thermal discharge and water quality in a 1,500-acre reservoir. *J. Water Pollut. Control Fed.* **42** (1), 24–32.

Cassie, D. 2006 The thermal regime of rivers: a review. *Freshwater Biol.* **51**, 1389–1406.

Chen, K. Q., Li, P. H. & Mi, X. B. 1999 The numerical simulation on impact of thermal discharge on eutrophication in lakes and reservoirs. *J. Hydraul. Eng.* **1** (1), 22–26 (in Chinese).

Deleersnijder, E., Campin, J. M. & Delhez, E. J. M. 2001 The concept of age in marine modelling: I. Theory and preliminary model results. *J. Mar. Syst.* **28** (3–4), 229–267.

Delhez, E. J. M., Campin, J. M. & Hirst, A. C. 1999 Toward a general theory of the age in ocean modeling. *Ocean Model.* **1**, 17–27.

Domagalski, J., Lin, C. & Luo, Y. 2007 Eutrophication study at the Panjiakou-Daheiting Reservoir system, northern Hebei Province, People's Republic of China: chlorophyll – a model and sources of phosphorus and nitrogen. *Agr. Water Manage.* **94**, 43–53.

Encina, L., Rodrıguez-Ruiz, A. & Granado-Lorencio, C. 2008 Distribution of common carp in a Spanish reservoir in relation to thermal loading from a nuclear power plant. *J. Therm. Biol.* **33** (8), 444–450.

He, M. F. 1997 Mechanism of water quality changes in Douhe Reservoir. *Water Resour. Protect.* **4**, 37–62 (in Chinese).

Jiang, C. L., Zhu, L. Q. & Hu, X. Q. 2010 Reasons and control of eutrophication in new reservoirs. In: *Eutrophication: Causes, Consequences and Control* (A. A. Ansari, G. S. Singh & G. R. Lanza, eds). Springer, Dordrecht, The Netherlands, pp. 325–340.

Li, Y. P., Acharya, K. & Chen, D. 2010 Modeling water ages and thermal structure of Lake Mead under changing water levels. *Lake Reserv. Manage.* **26** (4), 258–272.

Li, Y. P., Acharya, K. & Yu, Z. B. 2011 Modeling impacts of Yangtze River water transfer on water ages in Lake Taihu, China. *Ecol. Eng.* **37**, 325–334.

Li, P. H., Chen, K. Q. & Lu, G. S. 2001 Prediction of impacts of thermal discharge on eutrophication in Douhe Reservoir. *Water Resour. Protect.* **64**, 15–18 (in Chinese).

Liu, C. M. 1998 Environmental issues and the South-North Water Transfer Scheme. *China Q.* **156**, 899–910.

Liu, Z. T. & Cheng, B. F. 2011 Trends of changes in inflow of Douhe Reservoir and its influencing factors in the last decade. *Haihe Water Resour.* **4**, 36–28 (in Chinese).

Liu, Z., Wang, H. Y. & Guo, X. Y. 2012 The age of Yellow river water in the Bohai Sea. *J. Geophys. Res.* **117**, C11006

Lu, G. S., Li, P. H. & Tan, Z. S. 2001a Investigation of thermal impact and eutrophication and biological assessment for Douhe Reservoir. *Water Resour. Protect.* **63**, 26–30 (in Chinese).

Lu, G. S., Li, P. H. & Tan, Z. S. 2001b Analysis of eutrophication trend for Douhe Reservoir and remediation countermeasures. *Water Resour. Protect.* **65**, 22–25 (in Chinese).

Lucas, L. V., Thompson, J. K. & Brown, L. R. 2009 Why are diverse relationships observed between phytoplankton biomass and transport time? *Limnol. Oceanogr.* **54** (1), 381–390.

Monsen, N. E., Cloern, J. E. & Lucas, L. V. 2002 A comment on the use of flushing time, residence time, and age as transport time scales. *Limnol. Oceanogr.* **47** (5), 1545–1553.

Prats, J., Val, R. & Armengol, J. 2010 Temporal variability in the thermal regime of the lower Ebro River (Spain) and alteration due to anthropogenic factors. *J. Hydrol.* **387**, 105–118.

Refsgaard, J. C., Sørensen, H. R. & Mucha, I. 1998 An integrated model for the Danubian Lowland: methodology and applications. *Water Resour. Manage.* **12** (6), 433–465.

Shen, J. & Wang, H. V. 2007 Determining the age of water and long-term transport timescale of the Chesapeake Bay. *Estuar. Coast. Shelf Sci.* **74**, 585–598.

Shen, Y. M., Wang, J. H. & Zheng, B. H. 2011 Modeling study of residence time and water age in Dahuofang Reservoir in China. *Sci. China Phys. Mech. Astron.* **54** (1), 127–142.

Sheng, L. X., Liu, W. & Wang, Z. T. 1990 Effects of thermal pollution on aquatic environment and fish in Douhe Reservoir. *Acta Sci. Circumstantiae* **10** (4), 453–463 (in Chinese).

Sleigh, P. A., Gaskell, P. H. & Bersins, M. 1998 An unstructured finite-volume algorithm for predicting flow in rivers and estuaries. *Comput. Fluids* **27**, 479–508.

Smagorinsky, J. 1963 General circulation experiments with the primative equations, I. The basic experiment. *Mon. Weather Rev.* **91**, 99–164.

Straskraba, M., Tundisi, J. G. & Duncan, A. 1999 *Comparative Reservoir Limnology and Water Quality Management*. Kluwer Academic Publishers, Dordrecht, The Netherlands.

Takeoka, H. 1984 Fundamental concepts of exchange and transport time scales in a coastal sea. *Cont. Shelf Res.* **3** (3), 322–326.

Wang, G., Jiang, H., Xu, Z., Wang, L. & Yue, W. 2012 Evaluating the effect of land use changes on soil erosion and sediment yield using a grid-based distributed modelling approach. *Hydrol. Process.* **26**, 3579–3592.

Wang, G. & Xu, Z. 2011 Assessment on the function of reservoirs for flood control during typhoon seasons based on a distributed hydrological model. *Hydrol. Process.* **25**, 2506–2517.

Warren, I. R. & Bach, H. K. 1992 MIKE 21: a modelling system for estuaries, coastal waters and seas. *Environ. Model. Softw.* **7** (4), 229–240.

Xia, J., Zhang, L. & Liu, C. M. 2007 Towards better water security in North China. *Water Resour. Manage.* **21**, 233–247.

Zhang, S. M., Xu, Z. H. & Kong, K. 2011 Simulation and analysis on flow and pollutant of Jinan Queshan Reservoir. *CSISE* **105**, 693–699.

Zhao, D. H., Shen, H. W. & Tabils, G. O. 1994 Finite-volume two-dimensional unsteady-flow model for river basins. *J. Hydraul. Eng.-ASCE* **120** (7), 863–883.

First received 26 October 2012; accepted in revised form 25 February 2013. Available online 26 March 2013